SUPPLEMENTARY FIGURE LEGENDS

Supplementary Figure 1 (A) Yeast surface display system for the screening of antigen-binding scaffold libraries. vHHs are fused via its C-terminal to the N-terminus of Aga2p. Surface expression can be detected by using fluorescently labelled antibodies that bind the Myc tag. **(B)** Structural representation of vHH-Fc.

Supplementary Figure 2 The interaction between HZ-L-Yr-16 and 4-1BB, and different binding models of HZ-L-Yr-16 to 4-1BB. **(A)** The hydrophobic pocket of HZ-L-Yr-16, that grips the two β-sheets of CRD4 of 4-1BB. **(B)** The salt bridge interactions between HZ-L-Yr-16 and 4-1BB. HZ-L-Yr-16 and 4-1BB are colored cyan and green, respectively. The salt bridges are displayed as yellow dashed lines. **(C)** The conformational flexibility of 4-1BB in different ligand or antibody-bound structures. **(D)** The alignment of HZ-L-Yr-16/4-1BB structure with ligand-bound 4-1BB.

Supplementary Figure 3 Epitope bin comparison of HZ-L-Yr-16-Fc with Urelumab and Utomilumab. Control IgG or bispecific constructs were loaded onto AHC sensors, followed by blocking with an irrelevant IgG at 1 mg/mL. After a baseline step, the sensor was dipped into solution containing antigen (4-1BB), followed by testing of the antibodies or bispecific constructs to check for simultaneous binding. In the case of a non-competitor to the control IgG loaded onto the sensor, a strong binding curve should be observed. A competitor should not show any binding signal during this step.

Supplementary Figure 4 Characterization of HZ-C-Ye-18-Fc. **(A)** Binding of HZ-C-Ye-18-Fc to human PD-L1 overexpressing CHO cells measured by flow cytometry. **(B)** HZ-C-Ye-18-Fc blocking PD-1/PD-L1 interaction determined by flow cytometry. **(C)** HZ-C-Ye-18-Fc inhibits tumor growth in a MC38-huPD-L1 syngeneic mouse model. Data are mean ± SEM, *P<0.05.

Supplementary Figure 5 Epitope binding comparison of anti-PD-L1 antibodies. **(A)** Epitope binding comparison of HZ-C-Ye-18 (in purple), durvalumab (in orange), Atezolizumab (in cyan) and Avelumab (in green). **(B)** The alignment of PD-L1 with HZ-C-Ye-18 (in cyan), KN035 (in yellow; PDB: 5JDS) and PD-1 (in gray; PDB: 4ZQK). **(C)** The residues on PD-L1 interacting with HZ-C-Ye-18 (in cyan), KN035 (in yellow; PDB: 5JDS) and PD-1 (in gray; PDB: 4ZQK).

Supplementary Figure 6 Supplementary characterization of PM1003. **(A)** Affinity of PM1003 to human 4-1BB measured by BLI. **(B)** Affinity of PM1003 to human PD-L1 measured by BLI. **(C)** Binding of PM1003 to CHO cells measured by flow cytometry. **(D)** Binding of PM1003 to 293F cell measured by flow cytometry. **(E)** Simultaneous binding to both human PD-L1 and human 4-1BB of PM1003 measured by BLI. **(F)** PM1003-induced bridging of CHO-huPD-L1 cells and CHO-hu4-1BB cells.

Supplementary figure 1

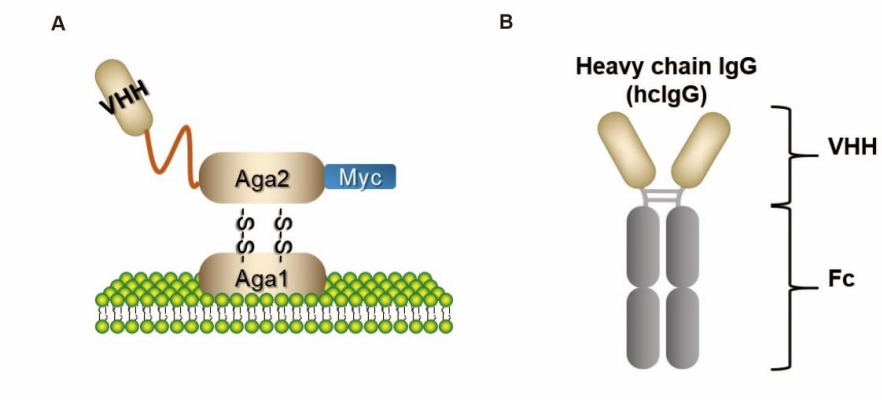

Supplementary figure 2

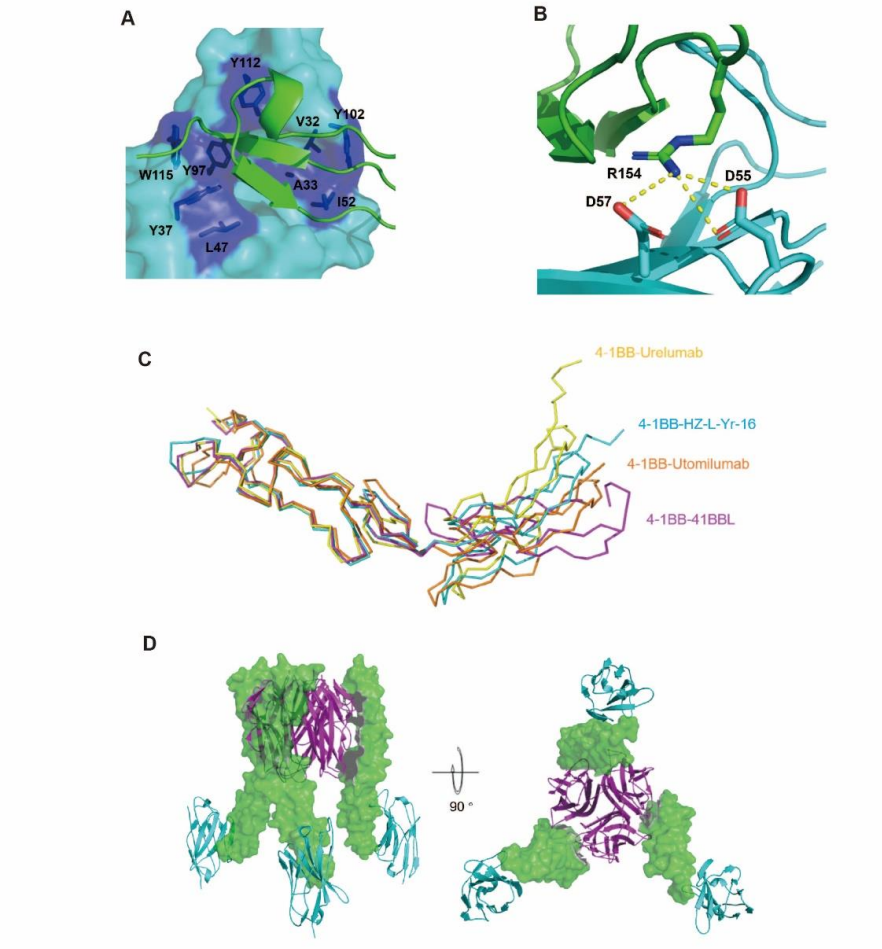

Supplementary figure 3

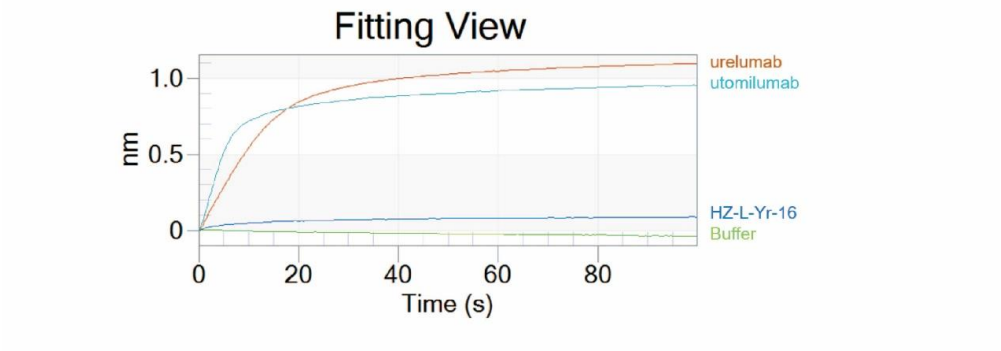

Supplementary figure 4

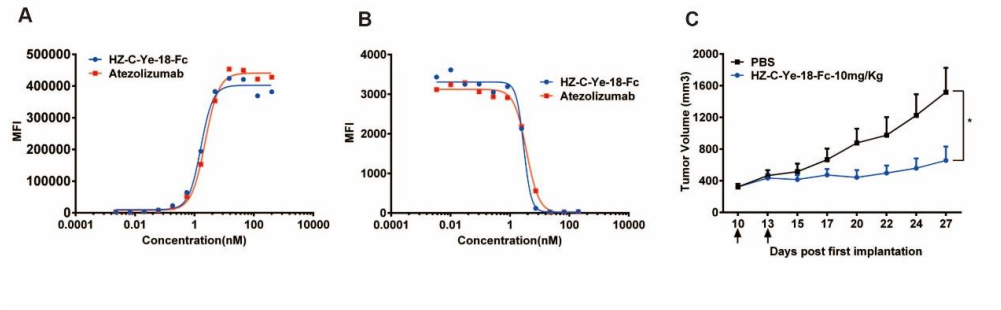

Supplementary figure 5

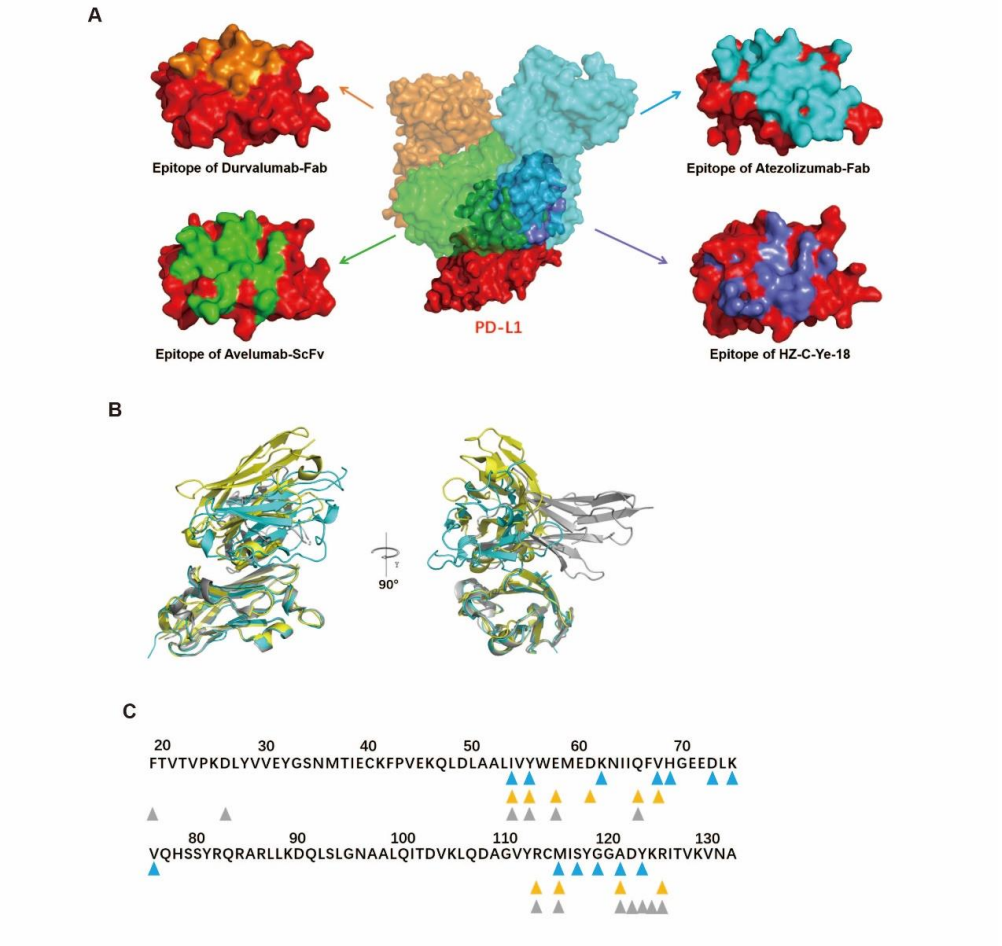

Supplementary figure 6

A

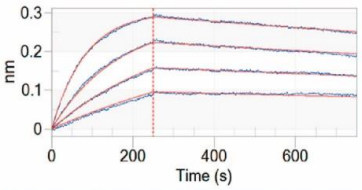

Antigen	K_D(M)	K_{on}(1/Ms)	K_{dis}(1/S)
4-1BB	4.90E-09	5.84E+04	2.87E-04

B

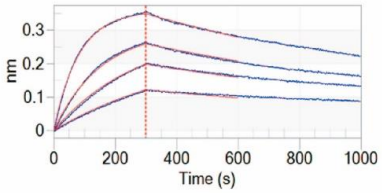

Antigen	K_D(M)	K_{on}(1/Ms)	K_{dis}(1/S)
PD-L1	1.60E-09	4.66E+05	7.47E-04

C

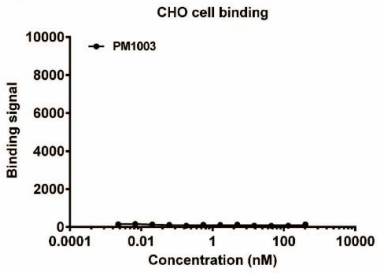

D

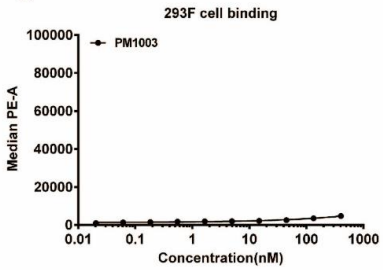

E

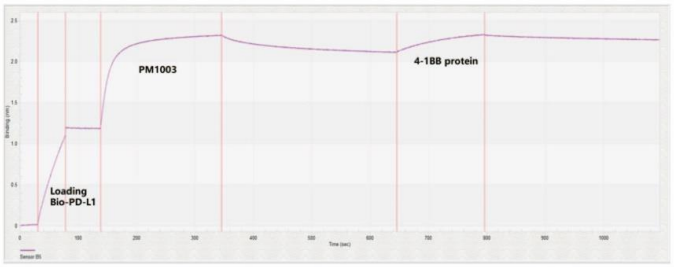

F

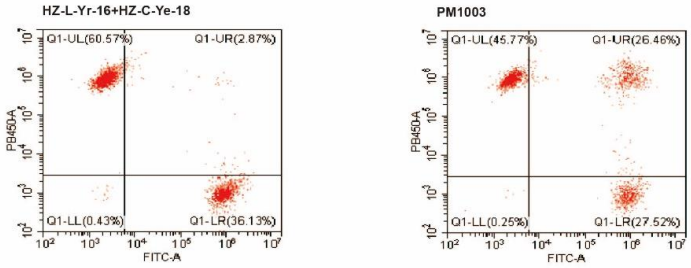

Supplementary table 1: Data collection and refinement statistics

	PD-L1:HZ-C-Ye-18	4-1BB:HZ-L-Yr-16
PDB entry code	7CZD	7D4B
Data collection[a]		
Space group	$P12_11$	$P4_12_12$
Cell dimensions		
a, b, c (Å)	34.62, 97.99, 67.52	106.85, 106.85, 146.41
α, β, γ (°)	90.00, 90.02, 90.00	90.00, 90.00, 90.00
Resolution (Å)	39.65 – 1.64 (1.67 – 1.64)[b]	47.79 – 3.14 (3.36 – 3.14)[b]
Rpim	0.031 (0.326)	0.047 (0.359)
I/σ I	15.0 (2.2)	16.1 (2.6)
Completeness (%)	94.6 (92.6)	99.9 (99.8)
Redundancy	3.5 (3.5)	12.9 (12.8)
Refinement		
Resolution (Å)	39.65 – 1.64 (1.68 – 1.64)	47.79 – 3.14 (3.22 – 3.14)
No. of reflections	49,377 (3529)	14,654 (1056)
R_{work}/R_{free}	0.150/0.184 (0.240/0.250)	0.211/0.258 (0.390/0.563)
No. of atoms		
Protein	3,758	2,029
Ligand/ion	31	146
Solvent	586	7
B-factors		
Protein	20.23	93.01
Ligand/ion	38.25	155.05
Solvent	30.62	61.15
R.m.s. deviations		
Bond lengths (Å)	0.004	0.012
Bind angles (°)	1.244	2.466
Ramachandran plot		
Favored (%)	97.0	95.0
Allowed (%)	3.0	4.0
Disallowed (%)	0.0	1.0

[a]A single crystal was used for data acquisition

[b]Values for the highest resolution shell are shown in parentheses